Холлівські двигуни є перспективним типом плазмового двигуна, який знайшов своє застосування в космосі. Незважаючи на це, з кожним роком відбувається зростання вимог до холлівських двигунів. Розробка нових сучасних моделей холлівських двигунів потребує вдосконалення теоретичної і діагностичної бази

Ключові слова: зіткненева випромінювальна модель, холлівський двигун з підрулюючим ефектом, оптична емісійна спектроскопія, плазма, температура електронів

Холловские двигателя являются перспективным типом плазменного двигателя, который нашел свое применение в космосе. Несмотря на это, с каждым годом отмечается рост требований к холловской двигателей. Разработка современных моделей холловской двигатели нуждается в совершенствовании теоретической и диагностической базы

Ключевые слова: столкновительная радиационная модель, холловский двигатель с подруливающим эффектом, оптическая эмиссионная спектроскопия, плазма, температура электронов

UDC 533.9.07
DOI: 10.15587/1729-4061.2017.96649

DEVELOPMENT OF XENON COLLISIONAL RADIATIVE MODEL FOR PLASMA DIAGNOSTICS OF HALL EFFECT THRUSTERS

R. Rajput*
E-mail: rajendrasurajput@gmail.com
A. Khaustova
Postgraduate Student*
E-mail: khaustova@khai.edu
A. Loyan
Senior Researcher*
E-mail: a.loyan@khai.edu
*Department of Electric Propulsion Thrusters
National Aerospace University
named after M. Zhukovsky Kharkiv Aviation Institute
Chkalova str., 17, Kharkiv, Ukraine, 61070

1. Introduction

Electric propulsion (EP) systems increasing use in terms of controlling commercial and military satellites is well known. Its application is demonstrated in station keeping, orbit raising, attitude control and de-orbiting at the end of satellites life [1]. The main interactive representatives of EP are Hall effect thrusters and ion thrusters. Considering other EP systems, these thrusters are competitive in terms of their performance and development cost. Its applicability is demonstrated for small to large class of satellite platforms.

Hall effect thrusters (HET) trend of use is increased because of its attractive characteristics. It has demonstrated high thrust to power ratio that allows rapid orbit transfer, capability of very good controllability of thrust, stable operations for long time and limited power supply requirement reduces EP systems dry mass [2].

In order to improve the thruster's performance and lifetime decades of efforts are made to understand the plasma physics. This is carried out by extracting the information of plasma parameters and correlating it, to the reference parameters (construction material and design) of the thruster as given in reference [2]. Similarly, the information of electron temperature (T_e) profile reveals the energetic plasma influence on thruster surface as reported in reference [3]. Further this effect of near wall T_e on thruster surface is confirmed with the erosion measurement [4]. Therefore the plasma diagnostic technique that offers precise and quick estimation of T_e is an attractive tool for investigating the plasma interaction with thruster surface. The main goal of work was to develop and demonstrate the applicability of C–R model along with optical emission spectroscopy (OES) for analysis of T_e in HET plasma.

2. Literature review and problem statement

From last 2 decades, there is increasing interest of OES for the HET plasma diagnostics. Intrusive diagnostic tools encounter several challenges like influence of hot plasma causes sputtering of sensitive elements. As a result, during the thruster near field measurements it often leads to experimental interruptions due to failure of its sensitive elements. Also there is difficulty in reaching the complicated regions of thrusters, complicated apparatus allows measurements only at predefined points, exhaustive technique of T_e extraction and the required voltage sweep results in higher experimental time and cost. In order to circumvent these complications, OES method is employed for T_e investigation. OES in correlation with C–R model helps to extract the information of T_e as demonstrated in reference [5]. The accuracy of the determined plasma parameter depends on the errors arising from the experimental sources [6] (OES) and C–R models design. Studies quantitatively specifying the errors inducing from C–R models design [7] are limited as previously the electron kinetic modeling efforts were based on theoretical codes which lead to large uncertainties in extracted plasma parameters. In order to calculate xenon emission cross sections different theoretical [8] and experimental approaches were employed in past. Employing the experimental cross sections [9] reduces the complexity of C–R model and also it eliminates the discrepancy resulting from the theoretical

assumptions. Feasibility of determining the T_e by using the xenon experimental cross sections is given in reference [10]. Many studies are performed to confirm the applicability of xenon C–R model for HET plasma, but using this technique further focus on investigating the thrusters plasma physics [3] are scarce.

3. The purpose and objectives of the study

The aim was to design and test the applicability of C–R model for determining the T_e in the Hall effect thruster plasma.

To achieve the goal it is necessary to solve the following tasks:

1. Designing the xenon collisional radiative model capable of developing the emission spectrum observed in HET plasma. It includes line intensity selection, analysis of excitation rate coefficient and line intensity modelling.

2. Kinetic models applicability testing includes obtaining experimental intensity ratio and applying it to C–R model for T_e extraction.

3. Validation of kinetic model.

4. Analyzing the discrepancy betweeen the OES and developed C–R model with normalized line intensity.

4. Collisional radiative model development

Collisional radiative model is a detailed modeling of excitation and de-excitation processes leading to optical emission of line intensity.

C–R model development includes several stages. First stage begins with the selection of line intensity sensitive for the plasma parameter of interest (T_e, electron density and species population). In second stage for accurately modeling of line intensity it is important to understand the nature of mechanisms and cascade transitions from higher states responsible for optical emission. Third stage consists study of collisional mechanisms resulting in optical emission of line intensity which are included in balance equation. Cross sections include the inherent transition details of line intensity. By employing the emisison cross section in fourth stage, the emission excitation rate coefficient of collisional mechanisms are derived. Further in fifth stage, the rate coefficients are applied in modeling the line intensity. Finally in sixth stage by comparing the intensity ratio of C–R model to the OES, T_e is extracted.

In first stage, T_e optimal sensitivity of line ratio of wavelength 823.16 nm and 828.01 nm is confirmed and validated with reference [10] at HET operational range.

Second step includes the detail study of line intensity transitions. Most intense xenon near infrared (NIR) region lines are associated from the $2p_i$ (Paschen notation) excited states. Xenon atoms from upper level ($5p^5 6p$) $2p_i$ configuration are decaying to the $1s_i$ ($5p^5 6s$) levels as shown in Fig. 1. The xenon line intensity 823.16 nm and 828.01 nm has some unique characteristics. Line intensities 823.16 nm has transition probability to $1s_5$ metastable level and 828.01 nm has probability of radiative transition to lower state of $1s_4$ level, which is optically coupled to ground state. Line intensity 823.16 nm requires threshold electron energy of 1.51 eV to excite from $1s_5$ level through stepwise excitation whereas from ground state it requires 9.82 eV. To achieve the optical emission of line intensity 828.01 nm ($2p_5$) with the excitation from ground state it requires threshold electron energy of 9.93 eV. As $2p_5$ is excited from ground state it requires high threshold energy. Whereas the $2p_6$ level has high transition probability from low metastable level as mostly the low energy electrons contribute to this process [10].

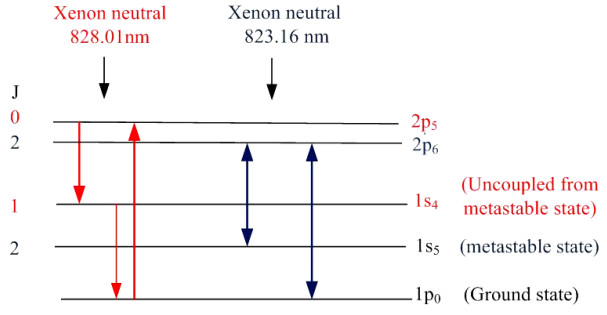

Fig. 1. In paschen notation electronic structure of Xenon atom is indicated for $5p^5 6p$ as $2p_i$ and $5p^5 6s$ is denoted as $1s_i$. J is the total angular momentum quantum number

Third stage includes the description of collisional mechanisms leading to optical emission of line intensity. As HET plasma is optically thin the reabsorption and pressure influences are very low as confirmed in reference [11]. It is evident from reference [10] that selected xenon NIR lines spontaneous emission rates meet the criteria to satisfy the condition of pure radiative decay in the HET discharge and plume region. Therefore it is justified that in HET plasma radiative decay of selected upper level dominate the other means of de-excitation. Population of the ion charge higher than Xe^{+2} is sufficiently low in HET plasma to be further considered in intensity modeling [4]. In order to reduce the complexity of C–R model, only dominant mechanisms involved in the optical emission of line intensity are included as shown in equation (1–4). By using the dominant collisional mechanisms, it is demonstrated in reference [10] that standard error of 11 % is observed in T_e determination. The symbol * indicates the excitation charge, Xe, Xe^+ and Xe^{+2} is xenon neutral atom, single and double ion charges respectively, m is metastable state and p indicates the upper excitation level.

Electron and neutral xenon atom collision:

$$e + Xe \rightarrow Xe^* + e. \quad (1)$$

Single ion and neutral collision:

$$Xe^+ + Xe \rightarrow Xe^{+*} + Xe^*. \quad (2)$$

Double ion and neutral collision:

$$Xe^{+2} + Xe \rightarrow Xe^{+2*} + Xe^*. \quad (3)$$

Stepwise excitation of metastable:

$$e + Xe \rightarrow Xe_m^* + e \ (m < p),$$

$$e + Xe_m^* \rightarrow Xe_p^* + e. \quad (4)$$

Equation (4), indicates the long life metastable atoms are formed as a result of collisions. Using equation (5), the optical emission intensity with the characteristic wavelength of

828.01 nm (uncoupled from metastable level), 823.16 nm and 834.68 nm can be calculated:

$$I^{\lambda}=\frac{hc}{4\pi\lambda}N_oN_e\left(k^{\lambda}_{eo}+\alpha\times k^{\lambda}_{+}+\left(\frac{1-\alpha}{2}\right)\times k^{\lambda}_{+2}\right)\left(1+\frac{k^{\lambda}(T_e)}{\zeta^{\lambda}}\right), \quad (5)$$

where I^{λ} is modeled line intensity, h is Planks constant, c is speed of light, λ is wavelength, N_e, N_o is number density of electron and neutral atoms, k^{λ}_{eo}, k^{λ}_{+}, k^{λ}_{+2} is the electron, first ion and second ion excitation rate coefficient, e is electron charge and $k^{\lambda}(T_e)/\zeta^{\lambda}$ is fractional increase in intensity due to metastable contribution:

$$\alpha=N_1/N_e, \quad (6)$$

where α is ratio of single ion density to electron density and N_1 is single ion density.

In fourth stage the electron excitation rate coefficients as a function of T_e were determined by using the cross sections (assuming Maxwellian electron energy distribution function) as proposed in reference [11]:

$$k^{\lambda}_{eo}=\langle f(E_e)\sigma_e(E_e)V_e\rangle_T, \quad (7)$$

where $f(E_e)$ is normalized electron energy distribution function, E_e is average electron energy, $\sigma(E_e)$ is the electron excitation emission cross sections and V_e is electron velocity:

$$k^{\lambda}_{+}=\sigma^{+}_{ion}(E_{ion})\sqrt{\frac{2\cdot E_{ion}}{m_{ion}}}, \quad (8)$$

$$k^{\lambda}_{+2}=\sigma^{+2}_{ion}(E_{ion})\sqrt{\frac{4\cdot E_{ion}}{m_{ion}}}, \quad (9)$$

where σ^{+}_{ion}, σ^{+2}_{ion} are the single and double ion emission cross sections, m_{ion} is mass of ion. By using equation (10)–(11), on the basis of upper state degeneracy the relative cross sections of $1s_5$ to $2p_i$ levels are employed for calculating the metastable excitation rate coefficient as given in reference [10]:

$$k^{\lambda}(T_e)=\frac{\sum_i\left(k^{i}_{oe}+\alpha\cdot k^{i}_{+}+\left[(1-\alpha)/2\right]\cdot k^{i}_{+2}\right)}{k^{\lambda}_{oe}+\alpha\cdot k^{\lambda}_{+}+\left[(1-\alpha)/2\right]\cdot k^{\lambda}_{+2}}, \quad (10)$$

$$\zeta^{\lambda}=\frac{\sum_i P_{r_i}T_i}{P_{\lambda}T_j}=\frac{\sum_i P_{r_i}(2J_i+1)}{P_{\lambda}(2J_j+1)}, \quad (11)$$

where P_{ri} and P_{λ} is the transition probability, T_i and T_j is excitation rate coefficient and J_i is total angular momentum quantum number.

In fifth stage by using the equation (5) optical emission intensity is modeled. And finally at sixth stage intensity ratio of lines with wavelengths 823.16 nm by 828.01 nm is modeled as a function of T_e as shown in equation (12). Further with regression model by comparing the intensity ratio of OES and C–R model the information of T_e is extracted accurately:

$$I^{R}(T_e)=\frac{\left(k^{823}_{oe}(T_e)+\alpha\cdot k^{823}_{+}(T_e)+\left[(1-\alpha)/2\right]\cdot k^{823}_{+2}(T_e)\right)\left(1+\frac{k^{823}(T_e)}{\zeta^{823}}\right)}{k^{828}_{oe}(T_e)+\alpha\cdot k^{828}_{+}(T_e)+\left[(1-\alpha)/2\right]\cdot k^{828}_{+2}(T_e)}, \quad (12)$$

Equation (12) can be employed for different plasma sources as shown in reference [7], by considering the variation of excitation rate coefficient of collisional processes in gas phase depending on the application of line intensity.

5. The results of the development and applicability of C–R model

For the diagnostics of the low power HET C–R model was developed previously and its applicability was demonstrated on SPT-20M8 [5]. The major difference between the previously developed C–R model [5] and model developed in this work is selection of line intensity ratio and associated processes sensitive for T_e range of interest.

By using equations (10–11), relative metastable contribution leading to optical emission of line intensity as a function of T_e is as shown in Fig. 2. Selected line intensities are optically coupled to the $1s_5$ level. It is evident from results that intensity enhancement due to metastable contribution ranges from 150 % to 300 % as observed from Fig. 2.

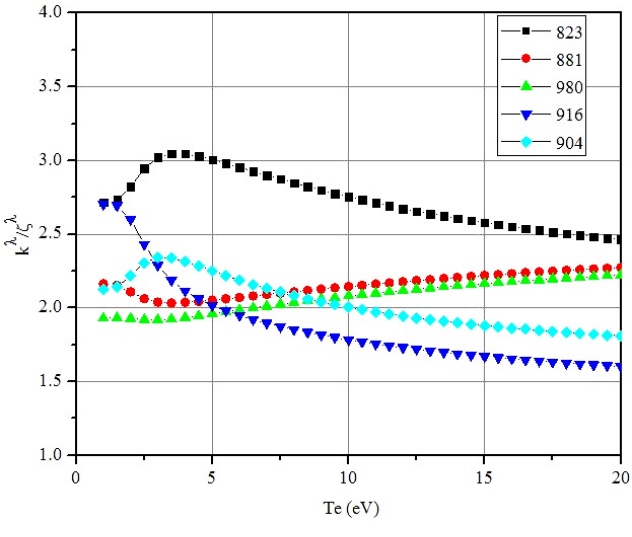

Fig. 2. Relative metastable excitation rate coefficient of xenon lines intensities as a function of T_e

In Fig. 3, the rate coefficients contributing to the line intensity of 823.16 nm are investigated as a function of T_e. It is observed that in the lower range of T_e (T_e<4.5 eV) metastable and ion contributions are dominant whereas at the higher T_e (T_e>4.5 eV) electron and metastable excitation has high contribution to optical emission of line intensity of wavelength 823.16 nm. It is observed from Fig. 1 (grotrian diagram), that the line intensity of wavelength 823.16 nm requires low threshold electron energy for stepwise excitation from $1s_5$ metastable level compared to its excitation from ground state [10]. As metastable excitation requires low threshold electron energy it has high population as observed from Fig. 3. Similar results are confirmed in reference [8].

Intensity ratio modeled with three electron kinetic models hypothesis as a function of T_e is shown in Fig. 4. Three models conditions are investigated i. e. intensity ratio modeled with metastable contribution, without metastable contribution and with corona model (CM). It is considered under CM that electrons have higher magnitude of velocity than the ion velocities. This results in the higher electron emission excitation

rate coefficients than the ion contribution. Therefore the line intensity modeled with corona model eliminates the heavy ion contributions. By comparing the line intensity ratio modeled with different hypothesis, it is observed from Fig. 4 that at lower T_e (T_e<4.5 eV) higher discrepancy occurs. Whereas at the higher T_e (T_e>4.5 eV) this discrepancy is reduced. Further it is confirmed from results that contribution of electron impact excitation increases with increasing of T_e as evident from CM and advanced C–R model (with metastable contribution) line intensity ratio overlap [4]. It is evident from Fig. 4, that intensity ratio of I^{823}/I^{828} is sensitive to the metastable contribution.

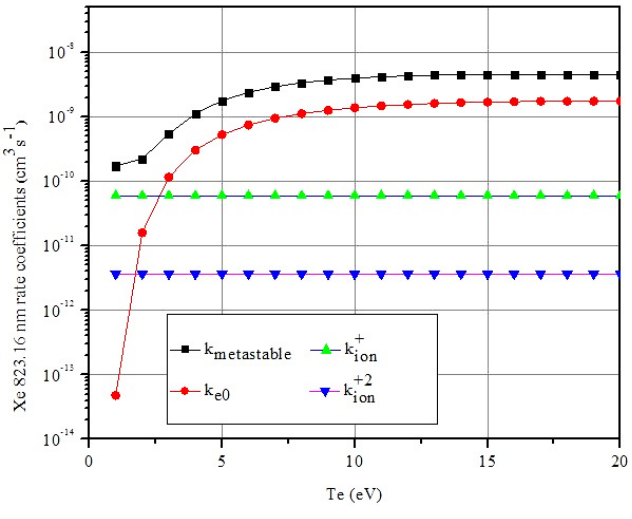

Fig. 3. Contribution of the rate coefficients as a function of T_e of line intensity with wavelength 823.16 nm

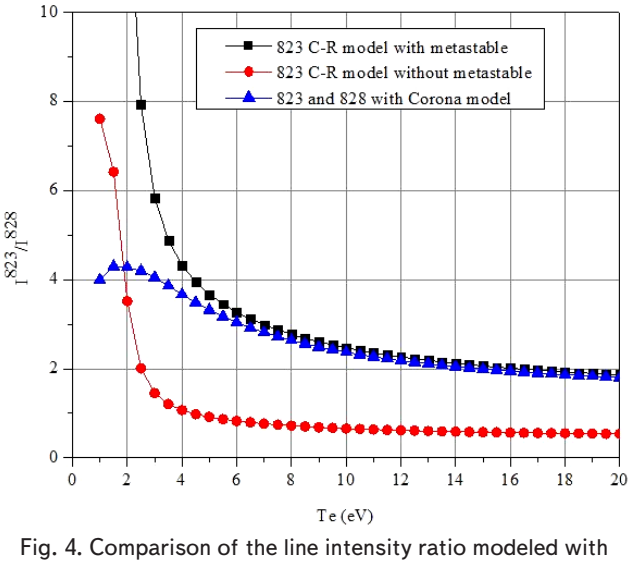

Fig. 4. Comparison of the line intensity ratio modeled with C–R model and CM as a function of T_e

In Table 1, T_e is determined by analyzing the OES intensity ratio (I^{823}/I^{828}) of 2.009 with three kinetic models hypothesis as shown in Fig. 4. The comparison of different kinetic models (as in Fig. 4) will signify the influence of models design on the accuracy of extracted T_e and confirms its applicability on HET plasma diagnostics. In the advanced C–R model, complete excitation mechanisms as given in equation (1–4) leading to optical emission of selected line intensity is included after careful analysis of transition levels. Further in order to determine the error in T_e measured with OES, there is need to confirm the result with probe measurements, which is not the interest of this article. Similar C–R model with metastable contribution is applied on HET in reference [13] and it is accepted that the error in measurements is lower than 15 %.

Second kinetic model represented as CM, it is also called as Corona model which excludes the Xe^{+} and Xe^{+2} ion contributions which are represented in equation (2–3). T_e determined with CM contributes to error of 24.57 %. The third simple C–R model eliminates the metastabe contribution as given in equation (4) for modeling the line intensity of 823.16 nm. By comparing the deviation of T_e results of CM and simple C–R model with the advanced C–R model errors are estimated. Errors of CM results are consistent with the radiance of ion contribution as reported in reference [10]. It is observed that by neglecting the metastable contribution the T_e is determined with 82.69 % of error, similar results are confirmed in reference [10]. T_e extracted with simple C–R model and CM, leads to under prediction of results with low accuracy. In Table 1, it is concluded from the experimental data that advanced C–R model with metastable contribution measures the T_e most accurately with error lower than 15 %. These results are confirmed at number of data points and so further the advanced C–R model will be applied for the HET plasma diagnostics.

Table 1

T_e is determined in HET discharge plasma with three kinetic models

Kinetic models	Advanced C–R model (with metastable)	CM (no ions)	Simple C–R model (no metastable)
T_e (eV)	15.98	14.45	2.73
Error (%)	<15 [13]	<24.57 [10]	82.69 [10]

The applicability of lines ratio I^{823}/I^{828} for investigating the T_e is demonstrated in reference [10]. In Fig. 5, the relative line intensity ratio is plotted obtained from designed C–R model and OES as a function of T_e. By comparing the experimental (OES) and C–R model intensity ratio it is confirmed that the line ratio is sensitive in the range of 1.8 eV to 30 eV. Latter, the linear dependence of the intensity ratio is observed till 70 eV. T_e above 1.8 eV upto the maximum range of 70 eV can be determined by using the selected line intensity ratio of I^{823}/I^{828}. OES experimental intensity ratio observed in near-field HET plasma as a function of T_e is shown in Fig. 5. Measurements are performed at 3 radial positions with T_e value of 14.37 eV, 16.13 eV, and 17.26 eV as shown in Fig. 5. Middle power HET tested in this work is investigated in the operational regime and investigation position similar to that of BPT-600 thruster. Range of near field T_e determined for the middle power HET is in agreement with the numerical T_e result reported in reference [14] for BPT-600 thruster.

Equation (13) is used to model the normalized line intensity where the intensity of each line is divided by sum of all lines:

$$I_{Nor} = \frac{I^{\lambda}_{Exp}}{\sum_i I^{i}_{Exp}} \approx \frac{I^{\lambda}_{C\text{-}R\ Model}}{\sum_i I^{i}_{C\text{-}R\ Model}}, \quad (13)$$

where I_{Nor}, I^{λ}_{Exp}, $I^{\lambda}_{C\text{-}R\ Model}$ are the normalized, experimental and C–R modeled line intensity, i is the number of line intensities included in the analysis.

Using equation (13) normalized line intensities of selected xenon NIR lines are shown in Fig. 6. OES and C–R model line intensities are measured at distance of 2 mm from thruster exit with discharge voltage of 300 V. It is observed from normalized line intensity that the errors arising from metastable approximation of wavelength 823.16 nm is 3.33 %, whereas for wavelength 828.01 nm which is uncoupled from metastable level it is about 18.10 %. Lower discrepancy (δ) is observed between experimental and C–R modeled normalized intensity. C–R model line intensities are in better agreement with value of α equal to 0.8 as shown in Fig. 6.

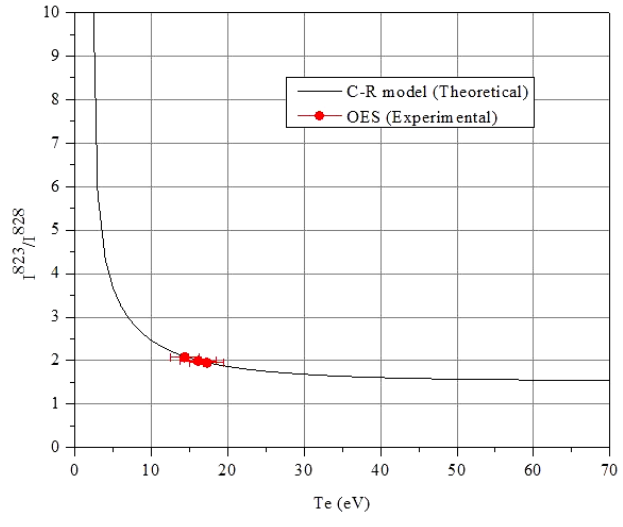

Fig. 5. Line intensity ratio of OES and C–R model of xenon wavelength 823.16 nm and 828.01 nm as a function of T_e

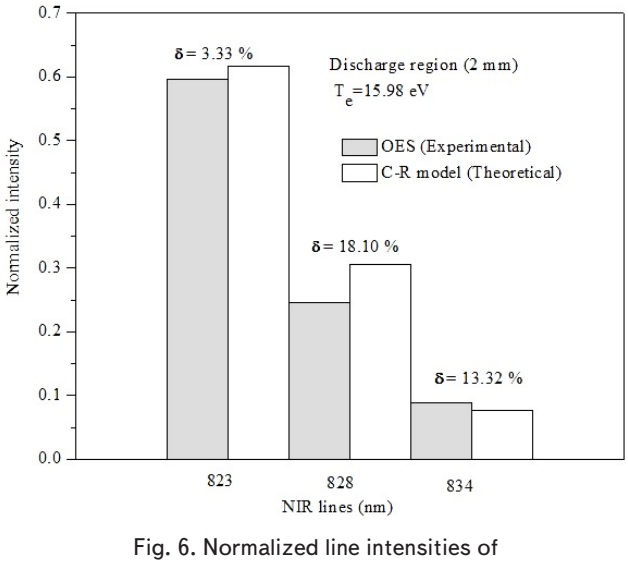

Fig. 6. Normalized line intensities of xenon NIR lines of interests

By employing the line intensity ratio method for T_e determination, sources of errors arises from the experimental and kinetic models design. Errors arising from the experimental sources are eliminated with researches performed in reference [6], although further uncertainty of 2.5 % is considered. In the designed kinetic model the means of error appears from the line intensity modeling and the method employed for the T_e extraction. By using the equation (14), the deviation between the experimental and C–R model line intensity ratio of I^{823}/I^{828} is analyzed. It is observed from the results that the line intensity ratio modeled with the designed C–R model with metastable contribution has error of 12.49 % at T_e value of 15.98 eV. Regression model is employed for extracting the T_e by correlating the OES and C–R model line intensity ratio. It is confirmed from the experimental results as reported in reference [5], that an error arising from regression model is lower than 1 %. So it is justified that the total error in the T_e determination is lower than 15 %, similar results are confirmed in the reference [13], in which the C–R model is applied on the GPT-1 thruster.

$$\text{Theoretical error} = \frac{\left(\frac{I^{823}_{Exp}}{I^{828}_{Exp}}\right) - \left(\frac{I^{823}_{C-R\ model}}{I^{828}_{C-R\ model}}\right)}{\left(\frac{I^{823}_{Exp}}{I^{828}_{Exp}}\right)} \times 100. \quad (14)$$

From test results it is predicted that by using the line intensity ratio I^{823}/I^{828} T_e is determined with error less than 15 %. It is evident from the lower discrepancy between the experimental and theoretical results that the C–R model is successfully designed and its applicability is confirmed for the HET plasma diagnostics.

6. Discussion of electron temperature and C–R model results

Feasibility of determining the T_e by using the C–R model in correlation with OES is demonstrated by investigating middle power Hall effect thruster plasma. This tool allows precise, stable and quick estimation of T_e in (1.8 eV to 70 eV) wide range of HET operation further it reduces the experimental time, complexity and cost. Accuracy of extracted T_e with line intensity ratio method applied in this work depends on errors arising from the OES (experimental sources) and C–R model (theoretical model) design. Errors arising from the experimental sources are eliminated as reported in reference [6]. Further to reduce the T_e uncertainties resulting from theoretical assumptions, NIR lines experimental cross sections were employed.

In order to simplify the electron kinetic model other assumptions were considered such as relative metastable excitation rate coefficient was employed as proposed in reference [10]. This further contributed for the error of 3.33 % as observed in modeling the line intensity of 823.16 nm. The range of T_e investigated using this kinetic model is limited from 1.8 eV to 70 eV.

The designed C–R model can be applied for the T_e diagnostic for the electric propulsion thruster propelled with xenon as propellant. This tool is attractive to perform the measurement in the critical areas of thruster as given in reference [13]. Importance of T_e information in HET plasma is discussed in section 1. This parameter can be used as reported in reference [3] for confirming the thruster design that reduced the interaction between energetic plasma and thruster surface. This diagnostics tool allows possibilities of studying the electron transport phenomenon in HET.

This model is applied to the middle power HET T_e investigation which results will be published in future. Further

research will be carried out to improve the measurements between experimental and theoretical model.

7. Conclusions

1. Xenon C–R model is designed and further by using the line intensity ratio I^{823}/I^{828} T_e is investigated in the middle power Hall effect thruster plasma.

2. Three kinetic models were tested for investigating the T_e in the range of 1.8 eV to 70 eV. It is concluded from results that I^{823}/I^{828} modeled with advanced C–R model that includes metastable contribution is applicable for the middle power HET plasma diagnostics.

3. Significance of collisional mechanisms is confirmed experimentally by comparing the T_e results obtained from three different electron kinetic models and the discrepancy of T_e is analyzed. It is confirmed that the T_e results are in good agreement with the BPT-600 thruster operating in same operational regime.

4. T_e is determined with error less than 15 %, as confirmed from normalized intensity results. Further by improving the line intensity modeling accuracy with C-R model and reducing error from OES, the extracted T_e accuracy can be improved.

Acknowledgement

The authors would like to thank the colleagues of Scientific Technological Center of Space Power and Engine, Ukraine for their guidance, patience and ideas.

References

1. Dudeck, M. Plasma propulsion for geostationary satellites and interplanetary spacecraft [Text] / M. Dudeck, F. Doveil, N. Arcis, S. Zurbach // Romanian Journal of Physics. – 2011. – Vol. 56. – P. 3–14.
2. Loyan, A. Performance Investigation of SPT-20M Low Power Hall effect Thruster [Text] / A. Loyan, T. Maksymenko // Proc. of 30th International Electric Propulsion Congress. – Florence, 2007.
3. Mikellides, I. Design of a Laboratory Hall Thruster with Magnetically Shielded Channel Walls, Phase III: Comparison of Theory with Experiment [Text] / I. Mikellides, I. Katz, R. Hofer, D. Goebel // 48th AIAA/ASME/SAE/ASEE Joint Propulsion Conference & Exhibit. – 2012. doi: 10.2514/6.2012-3789
4. Mikellides, I. Design of a Laboratory Hall Thruster with Magnetically Shielded Channel Walls, Phase I: Numerical Simulations [Text] / I. Mikellides, I. Katz, R. Hofer // 47th AIAA/ASME/SAE/ASEE Joint Propulsion Conference & Exhibit. – 2011. doi: 10.2514/6.2011-5809
5. Rajput, R. U. Plasma plume diagnostics of low power stationary plasma thruster (SPT-20M8) with collisional radiative model [Text] / R. U. Rajput, K. Aloyna, A. V. Loyan // The European Physical Journal Applied Physics. – 2017. doi: 10.1051/epjap/2017160348
6. Khaustova, A. N. Development of optical reciever for erosion rate measurements of gass discharge chamber external and internal ceramics separately [Text] / A. N. Khaustova, A. V. Loyan, O. P. Ribalov // Visnyk dvyhunobuduvannia. – 2015. – Issue 2. – P. 29–36.
7. Zhu, X.-M. Optical emission spectroscopy in low-temperature plasmas containing argon and nitrogen: determination of the electron temperature and density by the line-ratio method [Text] / X.-M. Zhu, Y.-K. Pu // Journal of Physics D: Applied Physics. – 2010. – Vol. 43, Issue 40. – P. 403001. doi: 10.1088/0022-3727/43/40/403001
8. Yang, J. Diagnosing on plasma plume from xenon Hall thruster with collisional-radiative model [Text] / J. Yang, S. Yokota, R. Kaneko, K. Komurasaki // Physics of Plasmas. – 2010. – Vol. 17, Issue 10. – P. 103504. doi: 10.1063/1.3486530
9. Borovik, A. Electron-impact ionization of xenon and tin ions [Text] / A. Borovik. – Giebe, 2010. – 206 p. – Available at: http://geb.uni-giessen.de/geb/volltexte/2011/8427/pdf/BorovikAlexander_2010_12_17.pdf
10. Karabadzhak, G. F. Passive optical diagnostic of Xe propelled Hall thrusters. II. Collisional-radiative model [Text] / G. F. Karabadzhak, Y. Chiu, R. A. Dressler // Journal of Applied Physics. – 2006. – Vol. 99, Issue 11. – P. 113305. doi: 10.1063/1.2195019
11. Chiu, Y. Passive optical diagnostic of Xe-propelled Hall thrusters. I. Emission cross sections [Text] / Y. Chiu, B. L. Austin, S. Williams, R. A. Dressler, G. F. Karabadzhak // Journal of Applied Physics. – 2006. – Vol. 99, Issue 11. – P. 113304. doi: 10.1063/1.2195018
12. Celik, M. Experimental and Computational Studies of Electric Thruster Plasma Radiation Emission [Text] / M. Celik. – Massachusetts Institute of Technology, 2007. – 240 p. – Available at: http://ssl.mit.edu/publications/theses/PhD-2007-CelikMurat.pdf
13. Spektor, R. Non-Invasive Plasma Diagnostic Inside A Hall Thruster Discharge [Text] / R. Spektor, E. J. Beiting // Proc. of 30th International Electric Propulsion Conference. – Florence, 2007.
14. Gonzales, A. Comparison of Numerical and Experimental Time-Resolved Near-Field Hall Thruster Plasma Properties [Text] / A. Gonzales, M. Scharfe, J. Koo, W. Hargus // 48th AIAA/ASME/SAE/ASEE Joint Propulsion Conference & Exhibit. – 2012. doi: 10.2514/6.2012-4197